Available online at www.sciencedirect.com
SCIENCE DIRECT®
Journal of Power Sources 139 (2005) 314–320
JOURNAL OF POWER SOURCES
www.elsevier.com/locate/jpowsour

Short communication

Porous silicon negative electrodes for rechargeable lithium batteries

Heon-Cheol Shin[a], James A. Corno[b], James L. Gole[b], Meilin Liu[a,*]

[a] *School of Materials Science and Engineering, Atlanta, GA 30332, USA*
[b] *School of Physics, Georgia Institute of Technology, Atlanta, GA 30332, USA*

Received 15 June 2004; accepted 29 June 2004
Available online 13 September 2004

Abstract

Porous silicon (PS) negative electrodes with one-dimensional (1-D) channels have been successfully fabricated using an electrochemical etching process. The peak current and the amount of charge transferred during cyclic voltametry (CV) increase with the channel depth of the PS, indicating that the channel wall of the PS participates in the lithiation/delithiation process. The channel structure of the PS electrodes remains essentially the same after 35 CV cycles in spite of the severe deformation of the channel wall during the repetitive lithium alloying/dealloying process. The specific capacity of the PS depends critically on the degree of activation of the PS before the galvanostatic charge/discharge experiment. For an exemplary PS electrode pre-activated by 20 CV cycles, the reversible specific capacity of the PS reached 43 μA h cm^{-2}. After a subsequent activation by 10 CV cycles, the capacity increased by 40% (60 μA h cm^{-2}). One-dimensional porous silicon appears to be a promising negative electrode for rechargeable micro-batteries.

Keywords: Porous silicon; Porous structure; Etching; Lithium battery

1. Introduction

Conventional micro-batteries have a two-dimensional (2-D) architecture with a parallel arrangement of a planar thin-film cathode and anode separated by a solid electrolyte. Unfortunately, the energy density and power density of 2-D batteries are mutually exclusive: with a decreasing thickness of the electrode, the power density is increased since the actual diffusion length of lithium through the thin-film electrode is reduced. However, the energy density is reduced because the fraction of the accompanying battery components such as the current collector, separator, and electrolyte is increased.

There has been widespread interest in three-dimensional (3-D) electrodes for the next generation design of a lithium micro-battery because of their great potential to achieve an improvement in both energy density and power density [1–3]. Three-dimensional electrodes in lithium batteries typically have active surfaces exposed to the electrolyte in three dimensions. Thus, the available volume of the active material can be much more effectively utilized, as compared to planar thin-film electrodes. More importantly, within the constraints of how uniformly the 3-D structure is created, the thicker the electrode, the larger will be the energy density (e.g., area specific capacity) without sacrificing power density.

Silicon can alloy with lithium electrochemically with up to 4.4 Li per Si, yielding an extremely large theoretical specific capacity of 4200 mA h g^{-1} [4,5]. Moreover, elemental Si shows a low voltage of <0.3 V versus Li/Li$^+$ [6], and high lithium ion diffusion coefficient ($\sim$7.2 $\times$ 10^{-5} cm^2 s^{-1} at 415 °C) [7]. Therefore, it is not surprising that there is considerable recent interest in Si-based electrode materials [8–13]. Recently, we have explored the possibility of using porous silicon (PS) as the negative electrode in rechargeable lithium batteries and have reported that the PS has a high reactivity with lithium at room temperature [14]. Nevertheless, the detailed characterization of the PS, including basic redox reactions, voltage profiles, and cycling stability has been lacking.

* Corresponding author. Tel.: +1 404 894 6114; fax: +1 404 894 9140.
E-mail address: melin.liu@mse.gatech.edu (M. Liu).

0378-7753/$ – see front matter © 2004 Elsevier B.V. All rights reserved.
doi:10.1016/j.jpowsour.2004.06.073

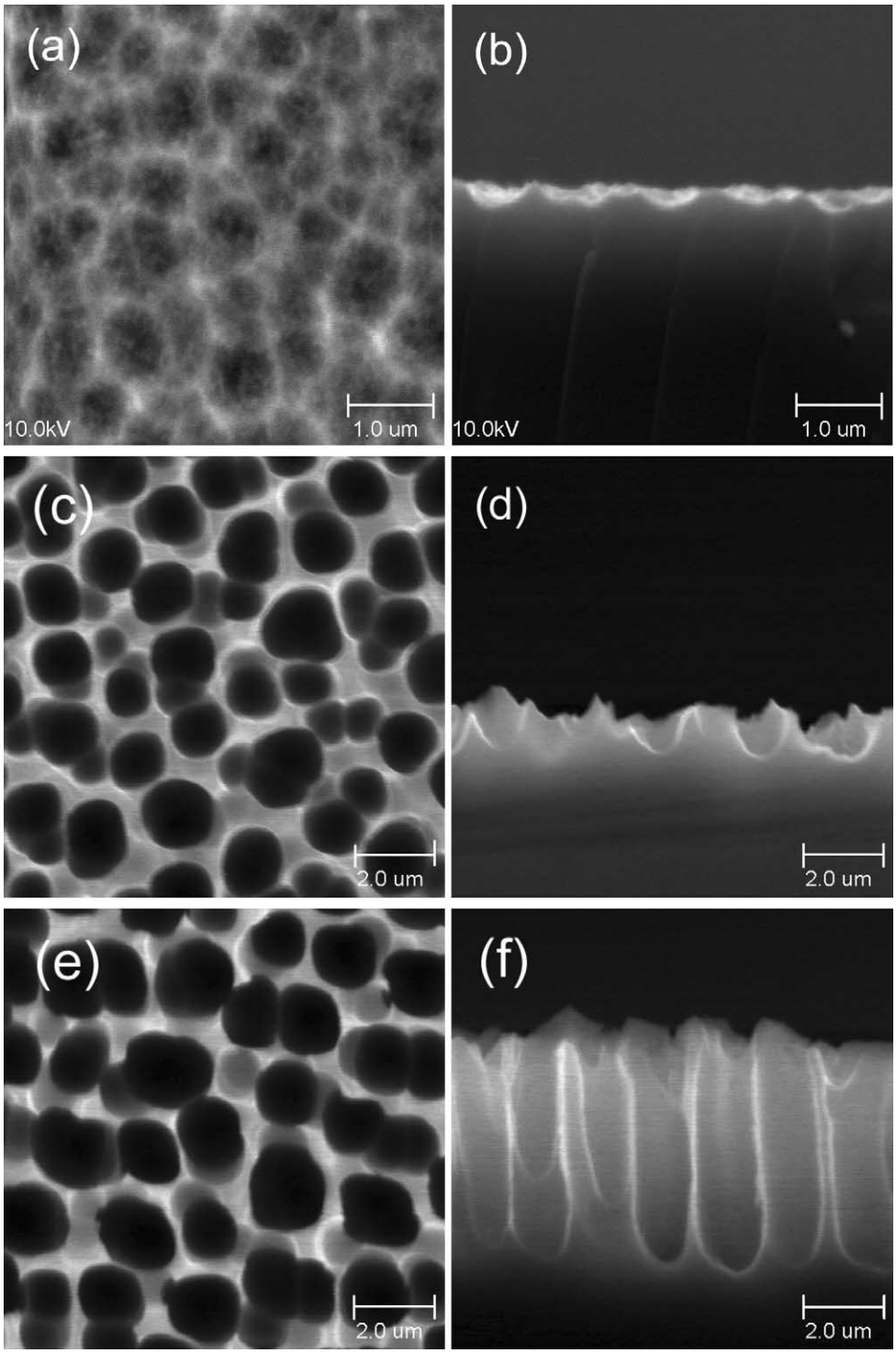

Fig. 1. Top (left) and cross-sectional view (right) of porous silicon (PS) electrodes with different channel depths, created by an electrochemical etching process; (a, b) was etched for 50 min; (c, d) and (e, f) are two separate regions of the same wafer etched for 40 min under the general conditions indicated in the experimental section.

In this work, we report the lithium storage characteristics of a variety of PS electrodes. Moreover, the critical factors affecting battery performance (e.g., specific capacity) will be discussed.

2. Experimental

For the majority of the experiments reported here, porous silicon was prepared using an acetronitrile (18 mL), TBAP (tetra-*n*-butylammoniumperchlorate, 1.2 g), and 49% HF (900 μL) solution placed in an electrochemical cell as described previously [15]. Silicon wafers (p-type; 1–20 Ω cm; 250–300 μm thick; 100 face orientation) were etched in a 5 cm^2 cell at a current of 20 mA. Platinum and an aluminum backing for the wafer were used as the counter electrode and current collector, respectively. After etching, the wafer was rinsed with methanol, dilute HF, dilute NaOH, and methylene chloride. It was then soaked for approximately 3 h in a 3 M HCl–methanol solution and rinsed with methanol again.

A two-electrode electrochemical cell (Hohsen test cell, Hohsen Corp. Japan) was employed for all electrochemical measurements. We used lithium foils as the counter electrode. The working electrode was as-prepared PS. Copper foil was mechanically bonded, as a current collector, to the backside of the PS. A Celgard 2400 separator, wetted with a 1 M solution of $LiPF_6$ in a 1:1 mixture of ethylene carbonate (EC) and diethyl carbonate (DEC), was sandwiched between the working electrode and counter electrode. The PS electrodes were cycled between 0.0 and 2.0 V versus Li/Li^+, using cyclic voltammetry. To evaluate the long-term cycleability of PS, the cells were galvanostatically charged and discharged in the voltage range of 0.1–2.0 V versus Li/Li^+ with a current density of 50 μA cm^{-2}. All the electrochemical experiments were performed using a Solartron 1285 potentiostat. All cells were assembled and tested in a glove box (VAC, USA) filled with purified argon gas.

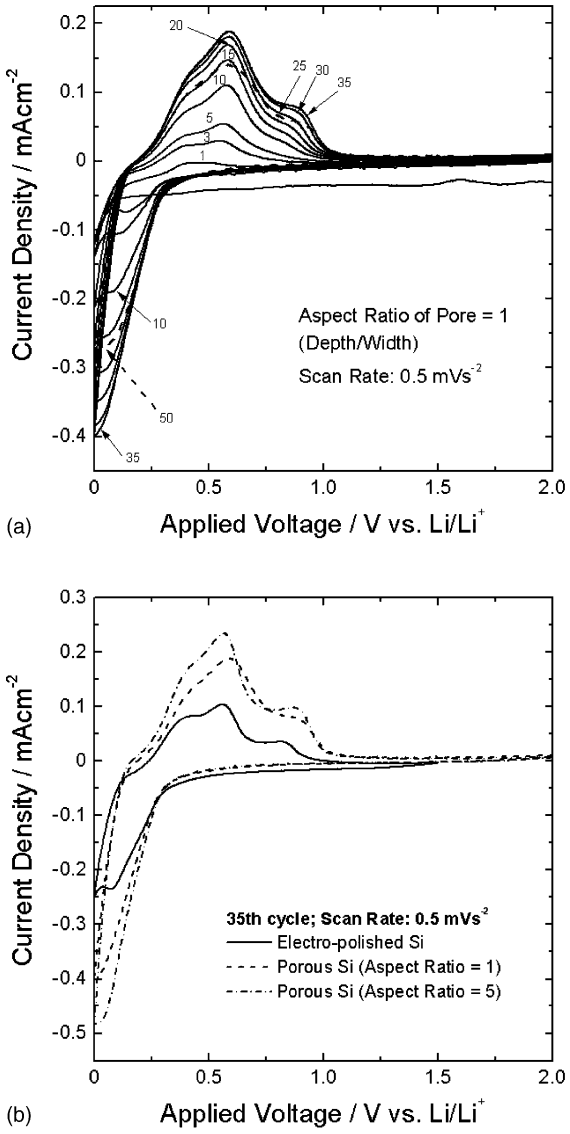

Fig. 2. (a) Typical cyclic voltammograms (CV) of the PS electrodes and (b) variation of the CV with the channel depth of the PS.

3. Results and discussion

Shown in Fig. 1 are surface views of the PS samples, created by an electrochemical etching process under different etching conditions. Apart from the electro-polished Si samples (Fig. 1a and b), the non-interconnected Si pores, formed perpendicular to the PS surface, were of order 1–1.5 μm in diameter. We anticipate that these channels will allow the penetration of liquid electrolyte and, therefore, that electrodes of this microstructure can facilitate a process producing high energy and power density.

Shown in Fig. 2a are the cyclic voltammograms of the PS electrode pictured in top and side view in Fig. 1c and d. It is noted that the current density and hence the charge transferred during the redox reactions increased (i.e., the electrode was activated) with cycling up to the 35th cycle. Following the 35th cycle, the current density decreased. The shape of the cyclic voltammograms and the activation process with cycling are consistent with a previous report on the cycling behavior of a structured silicon electrode formed as pillar arrays [16]. Considering that the lithium alloying/dealloying process results in significant internal structural changes (disorders) for the Si electrodes [9], the observed activation phenomenon is attributed to the reconstruction of crystal structure near the Si surface. Since it is expected that the rate of the reconstruction process is governed by the transport rate of lithium into crystalline silicon or the rate of amorphous Si–Li alloy formation, this kinetic bottleneck is likely to lead to the gradual activation of the PS electrodes at each CV cycle. On the other hand, the decrease in current density after approximately 35 cycles implies that the activation process competes with a simultaneous degradation process

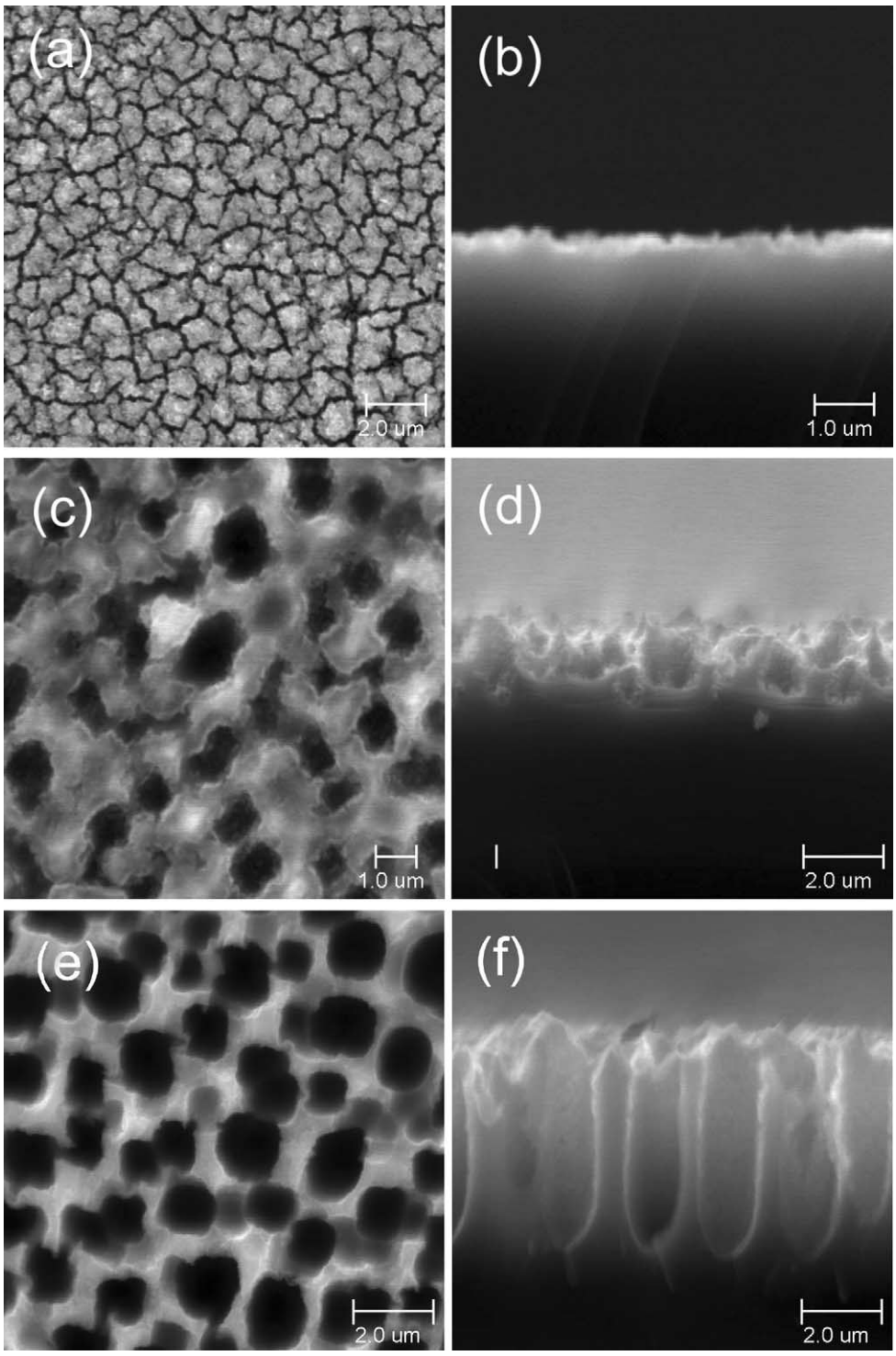

Fig. 3. The morphological change of the PS electrodes, pictured in Fig. 1 after 35 CV cycles.

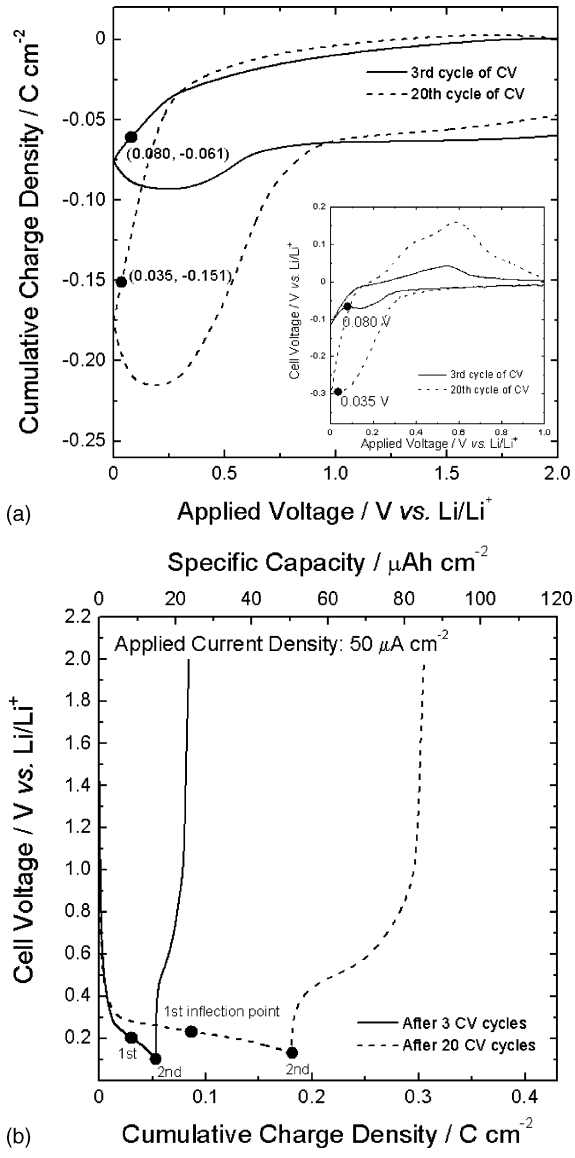

Fig. 4. (a) Cumulative charge density vs. applied voltage plots of the PS electrode (Fig. 1c and d), reproduced from the 3rd and 20th CVs (insert) and (b) voltage profiles of the PS samples after 3 and 20 CV cycles.

throughout the entire cycling process. After ∼35 cycles, the activation process is overwhelmed by the degradation process. Possible degradation mechanisms are (1) the mechanical disintegration of the Si during a significant volume change and (2) the irreversible capture of lithium ions by a significant number of insertion-generated defects inside the Si lattice [9].

Shown in Fig. 2b are the cyclic voltammograms of PS electrodes with different channel depths. It is noted that the peak current density increases with the PS channel depth, indicating that the channel wall of the PS participates in the lithiation/delithaition process. However, the peak current as well as the amount of charge transferred was not linearly proportional to the channel depth of the PS. In other words, the amount of charge transferred during the lithium alloying process with

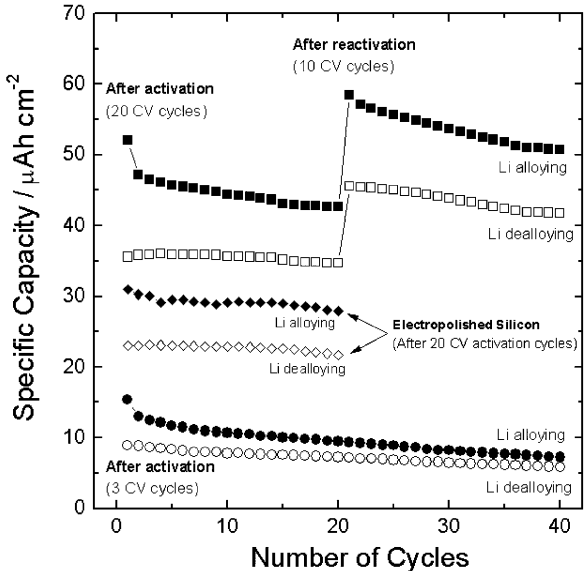

Fig. 5. Dependence of the specific capacity on the number of cycles at a current density of 50 μA h cm^{-2}, obtained from select PS electrode (Fig. 1c and d).

deep-channeled PS (aspect ratio = pore depth/diameter = 5) is just slightly higher than the amount of charge transferred by shallow-channeled PS (aspect ratio = 1). This indicates that, at this point, only part of the deep-channeled PS takes part in the lithium alloying/dealloying process. This postulation is supported by the microscopic images obtained for post-cycled PS, as shown in Fig. 3. Whereas the entire pore structure of the shallow-channeled PS has undergone a severe structural deformation during the repetitive lithium alloying/dealloying process only the top region (i.e., near the orifice) of the deep-channeled PS was found to be morphologically deformed, leaving the morphology of the deep region unchanged. One possible reason for the low utilization of the available active surface for the deep-channeled PS is the limited penetration of a viscous organic electrolyte into the porous structure, due to a strong capillary effect. From the SEM images, it is also noted that the porous structure of the PS electrodes remains essentially the same after 35 CV cycles (Fig. 3c and d) in spite of the severe deformation of the channel wall. For those samples of electro-polished Si, CV cycling produces a significant number of cracks in the surface (Fig. 3a and b).

Galvanostatic charge/discharge experiments were performed on the PS electrodes with two different electrochemical pre-treatments, 3 pre-CV cycles (sample A) and 20 pre-CV cycles (sample B). In order to avoid the catastrophic degradation of the PS electrodes accompanying the deep charging process (or lithium alloying), the lower cut-off voltages were carefully selected: Deep charging experiments have indicated that there is a very wide potential plateau below 0.1 V versus Li/Li$^+$ after the second inflection point on the voltage profile (data are not shown here). Therefore, we limited the lower cut-off for the potential to that point where the second inflection point on the voltage profile

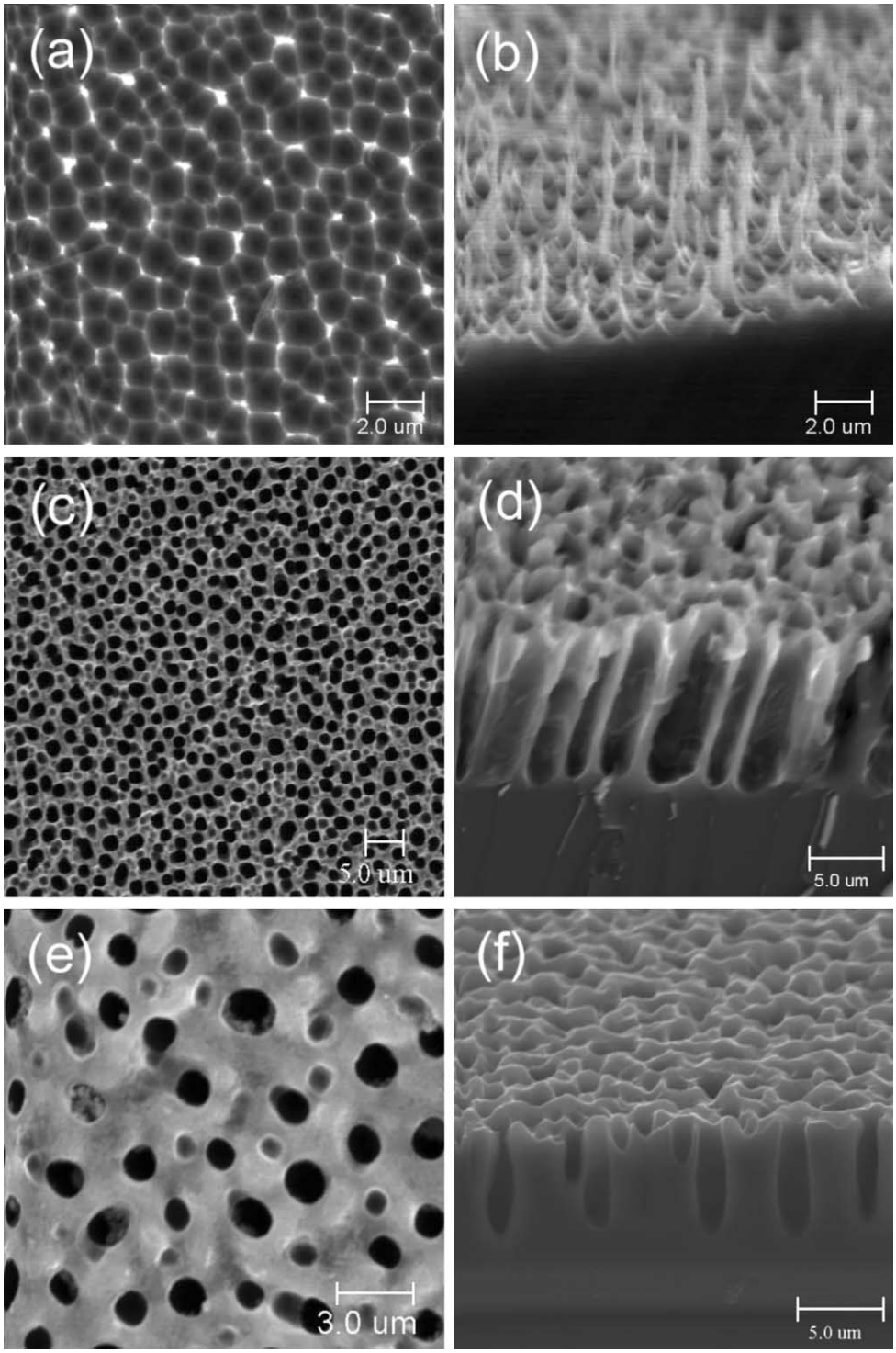

Fig. 6. Top (left) and cross-sectional view (right) of the PS electrodes with different pore densities, created by an electrochemical etching process; (a, b) was etched in HF (200 μL), TBAP (0.17 g), and MeCN (4.5 mL) at a current density of 20 mA cm^{-2} for 20 min and cleaned in dilute HF, ethanol, and doubly deionized water; (c, d) was etched in HF (200 μL), TBAP (6.66 g), and MeCN (5.5 mL) at a current density of 8 mA cm^{-2} for 60 min and then cleaned in dilute HF and hydrazine; (e, f) was etched for 40 min under the general conditions outlined in the experimental section.

begins to appear (typically around 0.1 V versus Li/Li^+), as shown in Fig. 4b. It is noted that the cathodic charge transferred during the charging process to the selected lower cut-off voltage coincides well with the cathodic charge transferred at the local maximum (or inflection point) of the cathodic branches of the CV, designated as solid circles in Fig. 4a and its insert. The initial specific charging capacities of the two samples A and B were 15 and 53 $\mu A\,h\,cm^{-2}$, respectively.

The cycling stability of samples A and B is shown in Fig. 5. Apart from the irreversible capacity fade during the first cycle, there is a relatively small capacity fade during subsequent charge/discharge cycles (0.5–1.0% per cycle). It is noted that the re-activation of sample B by 10 CV cycles (from 0.0 to 2.0 V versus Li/Li^+) increases the specific capacity by 40% (60 $\mu A\,h\,cm^{-2}$). This result strongly indicates that a lithium alloying reaction, occurring below ~0.1 V versus Li/Li^+, is responsible for the reconstruction (activation) of the PS electrodes for lithium storage. Nevertheless, the re-activation process appears detrimental to cycleability because the capacity fade becomes somewhat more severe after re-activation. On the other hand, the reversible capacity of the PS electrode is much higher than that of the electro-polished Si electrode (solid and open diamonds in Fig. 5), consistent with the CV results of Fig. 2b.

It is not easy to compare the specific capacity of our PS electrode with those in the literature (e.g., structured silicon formed as a pillar array [16]) because the size distribution, numerous coalescences of the pores, and the non-uniform thickness of the channel wall make a reasonable quantitative analysis (e.g., gravimetric capacity) for the PS electrodes quite difficult. Moreover, the strong dependence of the capacity on the electrochemical pre-treatment history complicates the situation. Nevertheless, in addition to its' cost-effectiveness and the ease of formation of active sites, our electrochemical etching technique has the potential to create a variety of morphologies with different rate capabilities and specific capacities. Using the current etching process, not only the pore depth (Fig. 1) but also the density of pores can be tunable. Shown in Fig. 6 are examples of PS electrodes with different pore densities, created under different etching conditions. The investigation of the effect of pore density on the electrochemical properties will be reported in subsequent communications.

One drawback of the present PS electrodes could be their low utilization of the deep-channel PS surface most likely resulting from penetrability of the electrolyte through the PS structure. The fabrication of a more desirable structure using a combination of chemical and/or electrochemical post-treatment of the PS samples (e.g., PS with a graded pore size and open orifice) for facile electrolyte penetration/ion transport is in progress.

4. Conclusion

Porous silicon created using an electrochemical etching process has been successfully used for the negative electrode in rechargeable lithium batteries. The capability for lithium storage improved with the increasing channel depth of the PS. Moreover, the porous structure remained essentially the same after charge/discharge cycling in spite of a severe volume change. The specific capacity ($\mu A\,h\,cm^{-2}$) of the PS electrodes increases with the degree of pre-activation at the expense of cycling stability, indicating that there is a trade-off between specific capacity and cycling stability. Thus PS, created by a relatively simple electrochemical etching process (versus for example, pillar formation), presents a new possibility for constructing a three-dimensional negative electrode that has significant potential for a high performance lithium micro-battery.

Acknowledgements

This work was supported by the Office of Science, Department of Energy under Grant No. DE-FG02-01ER15220.

References

[1] J.S. Sakamoto, B. Dunn, J. Mater. Chem. 12 (2002) 2859–2861.
[2] K. Kinoshita, X. Song, K. Kim, M. Inaba, J. Power Sources 81–82 (1999) 170–175.
[3] S. Ranganathan, R. Mccreery, S.M. Majji, M. Madou, J. Electrochem. Soc. 147 (2000) 277–282.
[4] M. Winter, J.O. Besenhard, M.E. Spahr, P. Noval, Adv. Mater. 10 (1998) 725–763.
[5] B.A. Boukamp, G.C. Lesh, R.A. Huggins, J. Electrochem. Soc. 128 (1981) 725–729.
[6] A. Anani, R.A. Huggins, J. Power Sources 38 (1992) 351–362.
[7] C.J. Wen, R.A. Huggins, J. Solid State Chem. 37 (1981) 271–278.
[8] S.B. Ng, J.Y. Lee, Z.L. Liu, J. Power Sources 94 (2001) 63–67.
[9] H. Li, X. Huang, L. Chen, G. Zhou, Z. Zhang, D. Yu, Y.J. Mo, N. Pei, Solid State Ionics 135 (2000) 181–191.
[10] H. Li, X. Huang, L. Chen, Z. Wu, Y. Liang, Electrochem. Solid State Lett. 2 (1999) 547–549.
[11] S. Bourderau, T. Brousse, D.M. Schleich, J. Power Sources 81–82 (1999) 233–236.
[12] W.J. Weydanz, M. Wohlfahrt-Mehrens, R.A. Huggins, J. Power Sources 81–82 (1999) 237–242.
[13] I.-S. Kim, P.N. Kumta, G.E. Blomgren, Electrochem. Solid State Lett. 3 (2000) 493–496.
[14] H.-C. Shin, Z. Shi, J. Gole, M. Liu, in: E. Wachman, K. Swider-Lyons, M.F. Carolan, F.H. Garzon, M. Liu, J.R. Stetter (Eds.), Solid State Ionic Devices III, The Electrochemical Society, Pennington, NJ, PV 2002-26, 2003, pp. 518–525.
[15] J.L. Gole, L.T. Seals, P.T. Lillehei, J. Electrochem. Soc. 147 (2000) 3785–3789.
[16] M. Green, E. Fielder, B. Scrosati, M. Wachtler, J.S. Moreno, Electrochem. Solid State Lett. 6 (2003) A75–A79.